

Characterisation of Li-Ion batteries by means of Bond Graph modelling

R. Saïssset *, **S. Astier ***, **C. Turpin ***, **B. Lafage ****

*Laboratoire d'Electrotechnique et d'électronique industrielle, LEEI - INPT - CNRS, 2 rue Camichel - 31071 Toulouse cedex 7 - France

astier@leei.enseeiht.fr

**Laboratoire de Génie Chimique, LGC - 18 chemin de la Loge - 31078 Toulouse cedex 4 - France

Abstract : In this paper, an original model of Li-Ion battery based on Bond Graph is described. Chemical, electrical and thermal aspects are considered together. It has been developed in order to perform simulations of complex power systems including power electronics and electrochemical components. Validation tests performed on a high power 37.5Ah accumulator developed for traction applications are presented.

1. Introduction

Advanced batteries are a growing \$40-billion-a-year business which substantially impacts the areas of energy storage, energy efficiency, and advanced autonomous systems such as in new ransport vehicles. Lightweight rechargeable Li-ion batteries are an attractive technology that offers the promise of higher energy densities than the ones currently available for power systems. In order to perform simulation studies of complex power systems such as hybrid vehicles including this type of storage we have developed a special new Bond Graph model which can be included in larger models of the whole system.

Chemical and electrical measurements made on a SAFT lithium ion accumulator cell of 37.5Ah and 3.5V [1] are used in order to validate this model on various test cycles.



Fig. 1. A view of the modelled and tested li-Ion battery cell

2. Bond Graph basics

Bond graph is an explicit unified graphical tool used to describe energy exchanges within a system and facilitating multidisciplinary modeling.

2.1 Bond Graph principles [5] [6]

In bond graphs, power interactions within a system are described by bonds. The bond is directed by half an arrow which arbitrarily indicates the positive power. Two variables, the effort e and the flow f , are associated to each bond, the product of which is the exchanged power.

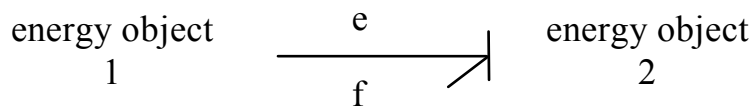


Fig. 1. Representation of the energy exchange by means of a bond

Though effort and flow have different interpretations in different physical domains, table 1, their product always is the transferred power. Furthermore, causality is a very useful concept in bond graphs as it is a fundamental feature in energy exchange. It establishes the cause and effect relationships between the factors of power. The causal bar indicates where the effort is imposed.

Table 1: Examples of effort and flow in various domains

Systems	e: effort (unit)	f: flow (unit)
Electrical	v: voltage (V)	i: current (A)
Mechanical	F: force (N)	V: velocity (m.s ⁻¹)
Chemical	μ : chemical potential (J. mol ⁻¹)	$\frac{dn}{dt}$: molar flow (mol.s ⁻¹)
Hydraulic	P: pressure (N)	$\frac{dq}{dt}$: volume flow (m ³ .s ⁻¹)
Thermal	T: temperature (K)	$\frac{ds}{dt}$: entropy flow (J.s ⁻¹)

2.2 Bond Graph standard elements

As indicated in Table II only a limited number of elements are necessary to describe the majority of physical systems.

Table 2: Bond graph elements

Element	Represents	Equation without causality
R:r	Resistance	$e - rf = 0$
I:i	Inertia	$e - i \frac{df}{dt} = 0$
C:c	Capacitance	$f - c \frac{de}{dt} = 0$
S _e	effort source	$e = cst$
MS _e	modulated effort source	$e = e(input)$
S _f	flow source	$f = cst$
MS _f	modulated flow source	$f = f(input)$

Energy flows are distributed by means junctions which connect elements together as indicated in Table III. There are two types of junctions : the one junction and the zero junction. Of course, elements connected together through a junction structure implies causality restrictions; for instance, an effort source (e.g. a voltage source) always determines the voltage at the 0-junction to which it is connected, and consequently to all other connected elements. The rest of the system determines the flow through this junction.

Table 1: Examples of effort and flow in various domains

Junction	Represents	Equation
1	equality of flows	$\sum_i e_i = 0$
0	equality of effort	$\sum_i f_i = 0$
TF	Transformer	$e_1 = re_2$ $f_2 = rf_1$
GY	Gyrator	$e_1 = rf_2$ $e_2 = rf_1$

3. Model of a Li-Ion accumulator Bond Graph basics

The figure 3 shows the structure of a Li-Ion cell. The cathode is a lithiated metal oxide (LiNiO₂.) and the anode is made of graphitic carbon with a layer structure. The electrolyte is made up of lithium salts (such as LiPF₆) dissolved in organic carbonates.

When the cell is being charged, the Lithium atoms in the cathode become ions and migrate through the electrolyte toward the carbon anode where they combine with electrons and are deposited between carbon layers as lithium atoms. This process is reversed during discharge.

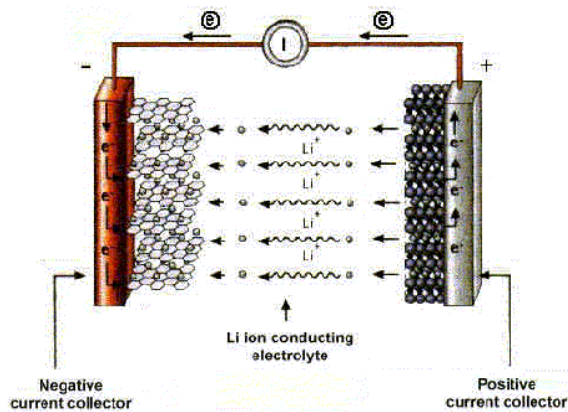


Fig. 3. Lithium-ion cell

With the aim to perform Bond Graph modeling, we have considered the several parts of this component as shown on figure 4.

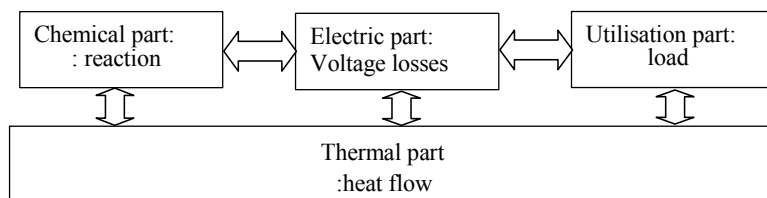


Fig. 4. Description of all fuel cell parts

Then, two model are possible : a model with two separated electrodes or a global equivalent one. As our accumulators doesn't enable us to test the electrodes separately for validation, we chose a model with one equivalent electrode. Moreover, thanks to the cylindrical shape of the accumulator, we could study half an accumulator. The fig.5 shows the chemical part of this model.

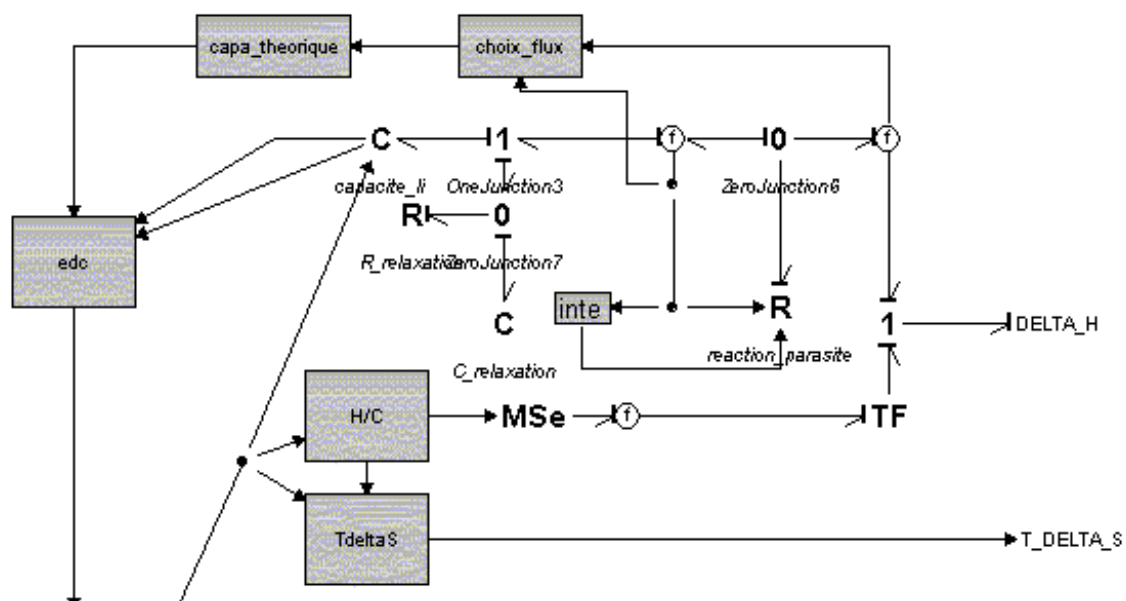


Fig. 5. Chemical part of lithium-ion battery

The nomenclature of variables used in the model is given at the end of the paper.

3.1 Chemical phenomena [2]

The enthalpy, entropy, and lithium mole number have to be determined by experiments. We measure the standard electromotive force at different temperatures.

$$\text{As } \Delta G^o = -E^o .n.F \text{ and } \delta S = \frac{dE}{dT} \quad (1)$$

ΔH of the reaction can be calculated.

During the charge and the discharge, transfer of lithium between electrodes gives the equation:

$$\Delta H = \Delta H^o + RT .\text{Log} \left(\frac{X_{\text{li}}}{X_{\text{li totale}} - X_{\text{li}}} \right) \quad (2)$$

X_{li} is the lithium quantity stored in the electrodes. In the model this storage is represented by a capacitor C1.

The lithium quantity is controlled by the molar flow. But there is a diffusion phenomenon in electrodes. Indeed, the concentration in each electrode is not uniform (figure 7,8). A concentration gradient modifies the ΔH . The RC circuit on Fig 4, represent the concentration in the electrode.

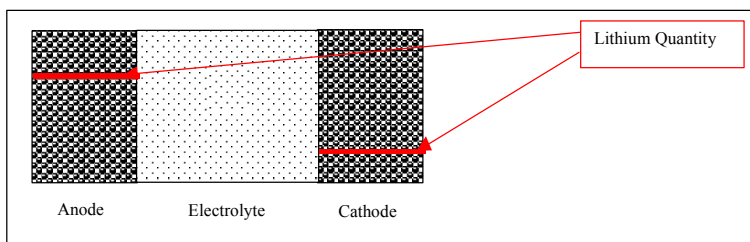


Fig. 7. Distribution of lithium in the electrodes at rest

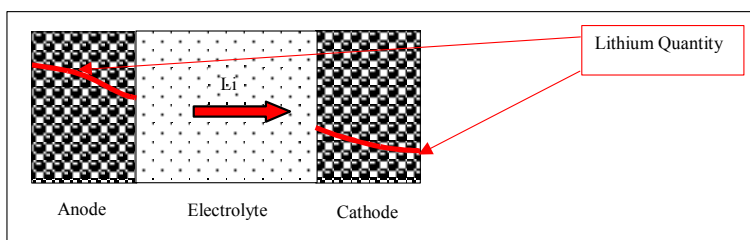


Fig. 8. Distribution of lithium in the electrodes during the discharge

Passing from chemical domain to electrical one is realised thanks to a transformer element TF. This transformer ratio is: $\frac{1}{n.F}$. Indeed, we know that the free energy of the reaction is transferred to exchanges electrons :

$$I = n.F .\xi \quad \text{and} \quad E^o = \frac{-\Delta G^o}{n.F} \quad (3) \quad (4)$$

3.2 Electric phenomena

Ohmic losses

There are ohmic losses in all electronic and ionic conductors. But, they are principally located within the electrolyte. Moreover, in our first approach we can consider a constant specific resistivity. So, resistance of electrolyte can be adequately described by:

$$R_e = \frac{l}{A \cdot \sigma} \quad (5)$$

Electrode voltage drop

The activation polarisation is present when the rate of electrochemical reaction at an electrode surface is controlled by sluggish electrode kinetics, which is described by Butler-Volmer equation.

Double layer capacitor

The double layer capacitor is established when an electronic conductor is in contact with an ionic conductor : a charge separation takes place on either sides of the interface. It can be identified with the frequency cut-off on the impedance diagram.

Then, the various voltage drops within an accumulator are given by a parallel circuit (RC) :

$$f_d = \frac{1}{2\pi \cdot R_t \cdot C_d} \quad \text{thus} \quad C_{da} = \frac{1}{f_d \cdot 2\pi \cdot R_t} \quad (6)$$

Deriving the Butler Volmer equation allows to identify R_t . But it is true only when current is near zero. Otherwise it is necessary to know the thickness of the ionic layer near the electrode. In general, it is about 0.5 to 1.5 nm.

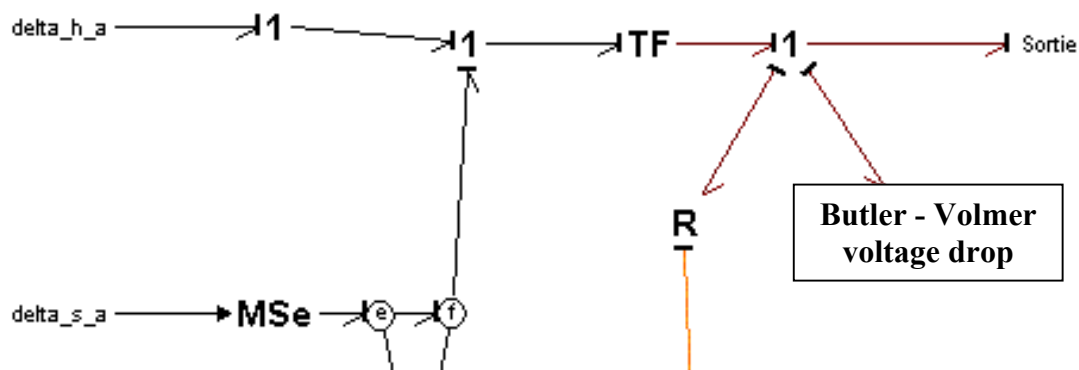
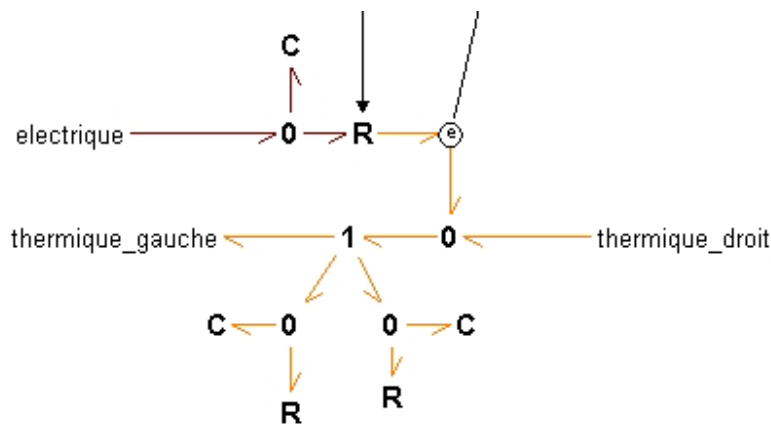


Fig. 9. Electric part of Lithium-ion battery

3.3 Thermal phenomena

We also have to consider thermal phenomena. We consider a one-directional transfer of heat : transversal in the cylinder. A battery is described as an association of cylinder connected in series. We suppose that the heat reaction is located on electrode. In Bond Graph method, temperatures are efforts and entropy flows are flows. Three power sources are present in the model : the reaction heat, the losses due to electrolyte resistance and the losses due to voltage drops (figure 10).



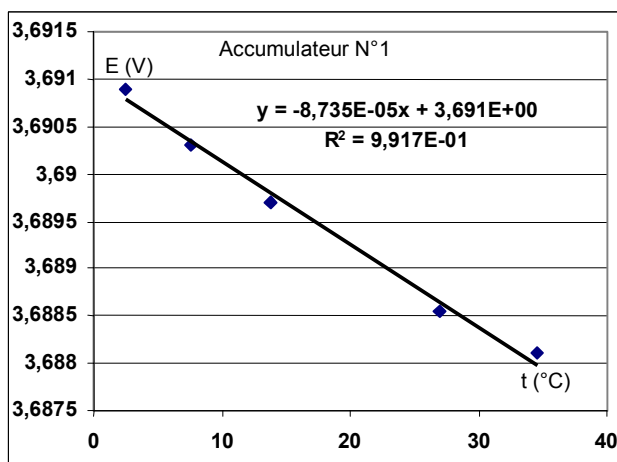
: Fig. 10. Thermal model of an electrode

4. Experimental validation [4]

4.1 Chemical test

Evaluation of coefficient $\frac{dE}{dT}$

From the E vs. Temperature plots, $\frac{dE}{dT}$ values can be determined, as shown in Fig. 11. We can observe the $\frac{dE}{dT}$ values determined at different depth of discharge for the considered cell.



$$\frac{dE}{dT} = -8.73 \cdot 10^{-5} \text{ V.K}^{-1}$$

$$\Delta S = -7.9 \text{ J.K}^{-1} \cdot \text{mole}^{-1}$$

Fig. 11. E vs. Temperature

For both cells, the entropy coefficient showed some dependence on the depth of discharge. This may be due to changes in the cell chemistry at different DOD. The negative dE/dT values indicate that the entropy heat effect is exothermic during discharge, and endothermic during charge, for all charge and discharge rates.

Efficiency

A cycle of charge and discharge have been performed between 3.3V and 3.9V, the voltage limits recommended by the manufacturer. The measurement of energy gives the efficiency of the accumulator. This efficiency is very good which confirms the very low entropy value.

	charge 1	discharge 2	Efficiency
Ah	26,38	26,83	
Wh	97,93	95,39	97,41

4.2 Electric test

The aim this test is to determine the three resistances of the model. The electrolyte resistance, the overpotential resistance and the relaxation resistance. Current interruption was used to measure the cell overvoltage at different depths of discharge. The discharge current was $I=15A$. It was not possible to take measurements at sampling rate higher than 0.1 s because of instrument limitations. The results is shown on fig. 11. The instantaneous voltage drop is mainly due to the ohmic resistance of the cell and partially due to the concentration polarization. The voltage drop due to ohmic resistance is a very fast process, characteristic of electron flows that take place in picoseconds. A high-frequency data acquisition system at MHz or an oscilloscope is required to capture the actual ohmic voltage drop in this step. The relaxation voltage drop is mainly due to concentration polarization in the liquid electrolyte and in the solid electrode materials. Especially the latter is a very slow process, characteristic of solid state ionic diffusion. The instantaneous impedance R_i and the relaxation impedance R_p were estimated using Eqs. 7 and 8 , respectively.

$$R_i = \frac{\Delta V_i}{I} \quad \text{thus} \quad R_p = \frac{\Delta V_p}{I} \quad (7) (8)$$

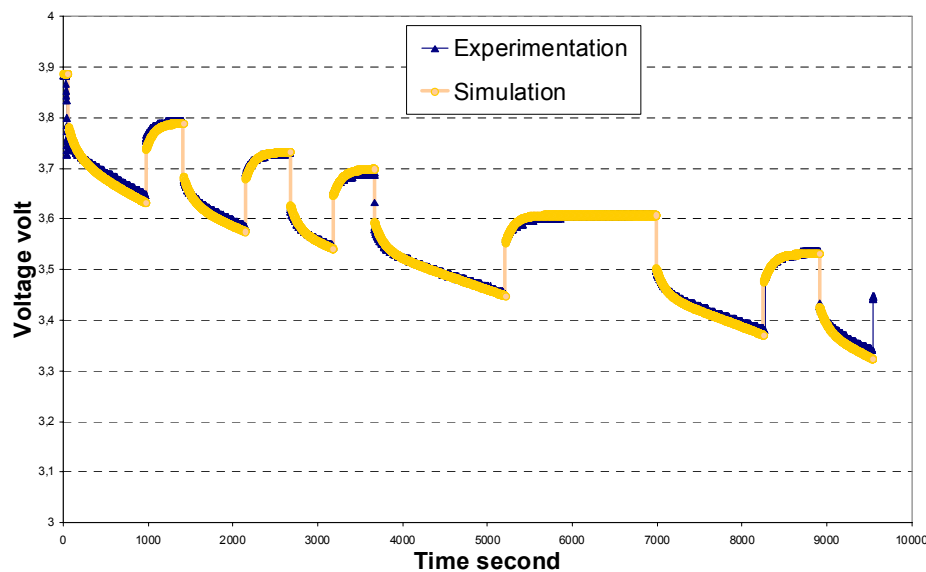


Fig. 11. Discharge with current interruptions

Then we can estimate the ohmic resistance during this discharge with the equation 8:

$$R_e = 0.007 \, \Omega$$

Another resistance value was estimated with an oscilloscope on 10A current interruptions as shown on Fig 12 giving :

$$R_e = 0.0054 \, \Omega$$

On fig 12, we can observe the effect of the double layer capacitor. The current interruption time constant of this effect is 20 ms

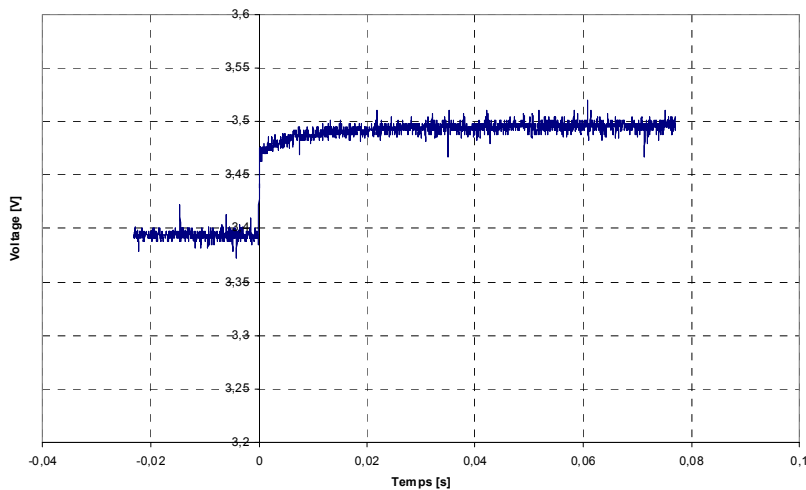


Fig. 12. Experimental effect of the double layer capacitor

On fig 13, the relaxation phenomenon is the most important. The time constant is 2000s.

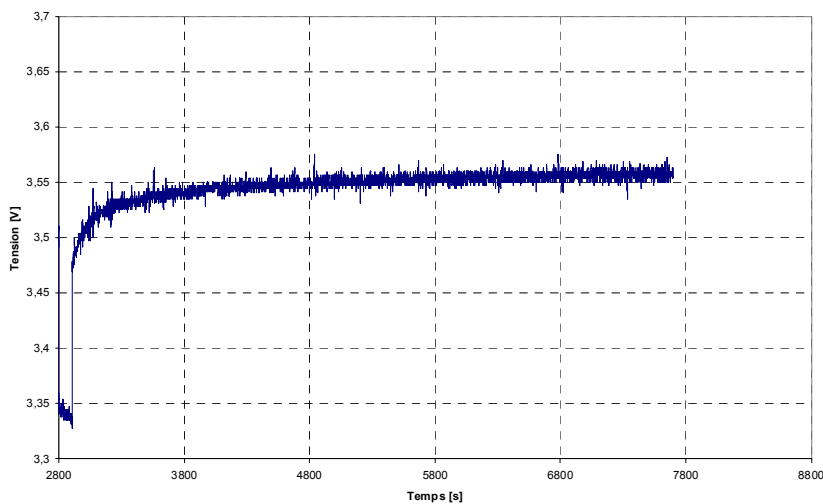


Fig. 13. Experimental relaxation measurements

Then we can notice three time scales in the accumulator. The scale of the ohmic resistance, the overpotential and the relaxation of the lithium in the electrodes. The model takes into account these different phenomena.

In order to validate this model, we have simulated and tested a charge at 7A with current interruptions. We can see that the model give an error inferior of 1%.

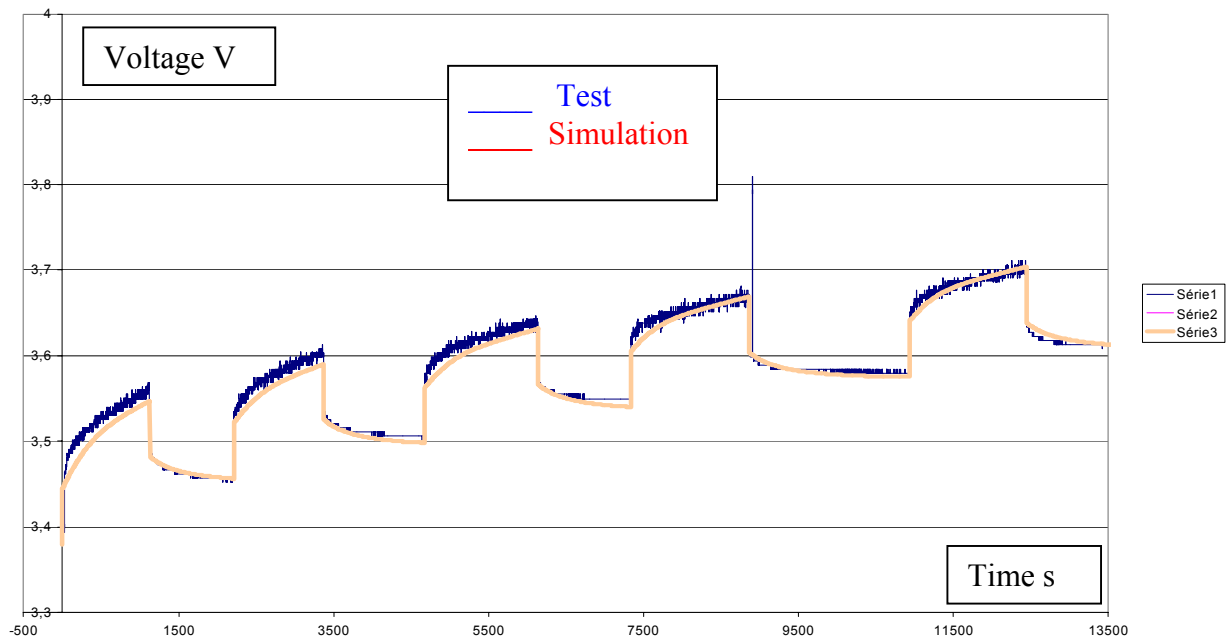


Fig. 11. Charge of an accumulator

5. Conclusion

The new Bond Graph model described in this paper represents the chemical and electrical phenomena in a lithium-ion battery. It was validated thanks to significant tests and is very useful for power electronic engineers. Indeed it can be inserted in larger models of complex systems including such elements. We use it in a more global model for electric car studies. Moreover, this model also enables to represent other chemical generators as fuel cell with few modifications [4] in the scheme above.

6. References

- [1] SAFT Documentation
- [2] I.PRIGOGINE D.KONDEPUDI, « Thermodynamique : Des moteurs thermiques aux structures dissipatives », *Edition Odile jacob, 1999*
- [3] R.SAÏSSET, C.TURPIN, S. ASTIER, B. LAFAGE “Study of Thermal Imbalances in Arrangements of Solid Oxide Fuel Cells by mean of Bond Graph Modelling” *Power Electronics Specialist Conference 2002*
- [4] S. AL HALLAJ, “Characterization of commercial Li-ion batteries using electrochemical calorimetric measurements” *Journal of power sources, 1999*
- [5] H.PAYNTER, “Analysis and design of engineering systems”, MIT Press, 1961
- [6] D.KARNOPP, R.ROSENBERG, “Systems dynamics : a unified approach”, John Wiley & Sons, 1991

Nomenclature used in the model

R	universal gas constant	$8.314\text{J}\cdot\text{mol}^{-1}\cdot\text{K}^{-1}$
T	internal temperature	Kelvin
Text	external temperature	300K
n	mole number in reaction	2
F	Faraday constant	96493C per eq.
ΔG°	free energy	
Cda	anodic double layer capacitor	μF
Rta	anodic overpotential resistance	Ω
Cdc	cathodic double layer capacitor	$m\text{F}$
Rtc	cathodic overpotential resistor	Ω
E°	standard electromotive force	volt
U	voltage	
I	current	
ξ	molar flow	mol/s
Re	electrolyte resistance	ohm
l	electrolyte length	μm
A	geometric area of cell	cm^2
iao	anodic current	A
ila	anodic limit current	A
ilc	cathodic limit current	A
α_1 and β_1 :transfer coefficients with $\alpha_1+\beta_1=1$.		
η_a	anodic overpotential	V
η_c	Cathodic overpotential	V
X_{Li}	Lithium quantity	Mol
X_{lithium}	Lithium quantity in electrode	Mol
L	Electrolyte Length	M
A	Electrolyte Area	M^2
σ	Electrolyte conductivity	$(\Omega\text{m})^{-1}$